Nucleus-nucleus collisions in the dynamical string model

B. Iványi,[1,2] Z. Schram,[1] K. Sailer,[1] and G. Soff[2]
[1]*Department for Theoretical Physics, Kossuth Lajos University, H-4010 Debrecen, Pf. 5, Hungary*
[2]*Institute for Theoretical Physics, Technical University, D-01062 Dresden, Germany*
(Received 12 January 1999; revised manuscript received 19 August 1999; published 19 January 2000)

In this paper the dynamical string model is applied to the numerical simulation of the ultrarelativistic heavy-ion collision ^{32}S(200 GeV/nucleon)+^{32}S. The results are in qualitative agreement with experimental data.

PACS number(s): 25.75.−q, 24.85.+p

I. INTRODUCTION

The purpose of the present paper is to show that the dynamical string model offers an alternative approach to describe ultrarelativistic heavy-ion collisions at bombarding energies of a few hundreds GeV/nucleon in terms of extended objects, the so-called hadronic strings.

The existing event generators for high-energy hadronization processes can be classified as follows.

(1) Event generators for a high-precision description of elementary hadronization processes (including only lepton and proton beams) in a vacuum: PYTHIA [1], HERWIG [2], ARIADNE [3], LEPTO [4], and ISAJET [5]. These event generators combine the parton-shower evolution in perturbative QCD terms with a nonperturbative hadronization prescription to convert final partonic distributions into hadronic ones. For the latter, the LUND string fragmentation model is commonly used [6], with the exception of HERWIG, which uses other considerations for coalescing colored partons to color-neutral clusters and fragmenting those into hadrons. The common feature of this class of models is the lack of space-time evolution. Therefore, these models cannot be directly applied for describing hadronization at finite densities, e.g., for that of high-energy hadronization processes involving also nuclei.

(2) Event generators for the description of hadronization at finite densities, e.g., high-energy heavy-ion collisions: FRITIOF [7], PCM [8], DPM [9], VENUS [10], QGSM [11], RQMD [12], UrQMD [13], HSD [14], HIJET [15], and HIJING [16]; two-phase simulation of ultrarelativistic nuclear collisions [17].

These models provide a space-time description (except HIJING) of the hadronization process considered. In a few of them [8,9,17,16], the partonic degrees of freedom are included also in the early stage of the collision in some form. Hadrons are generally treated as point particles with interaction ranges prescribed on the base of the constituent valence-quark picture. As a rule, string excitation is included (with the exception of [17]) in various forms and the LUND string fragmentation model [6] is used. Generally, stringlike excited hadronic states do not propagate and collide with other hadrons in their surroundings. Strings are rather a clever tool of bookkeeping how highly excited hadrons fragment into hadrons of the discrete mass spectrum.

(3) Models which intend to provide a space-time description for both the high-energy elementary hadronization processes in a vacuum and the more involved hadronization processes at finite densities, such as those including nuclei, e.g., VNI [18]. VNI gives a full space-time picture of ultrarelativistic heavy-ion collisions, combining the space-time evolution of the parton shower in its early stage with the later hadronic cascade. The space-time picture of the parton cascade has also been used in the parton-hadron conversion, based on the ideas introduced in [2]. There are no strings in this model, the hadrons are considered point particles with finite interaction ranges, as usual.

The dynamical string model presented here belongs to the third class of models providing a full space-time description. It can be applied to elementary hadronization processes in a vacuum and to hadronization processes at finite densities involving nuclei as well. It is the basic feature of the dynamical string model that during the whole space-time evolution of an event all the hadrons are consistently considered extended, stringlike objects satisfying the particular laws of string dynamics. Contrary to other models on the market, the string picture is not merely used as a fragmentation model of excited hadrons. It is taken here as the model for hadron dynamics, according to which the laws of motion, decay, and collision of hadrons are determined.

Contrary to the models, including a parton shower, for the early stage of the evolution, the dynamical string model considers the stringlike collective excitations of the hadrons to be decisive for the evolution of the ultrarelativistic heavy-ion collision, neglecting completely the underlying partonic processes. The good qualitative description of ultrarelativistic heavy-ion collisions for CERN Super Proton Synchrotron (SPS) energies of a few hundreds GeV/nucleon obtained in the present paper indicates that the overall qualitative features of the fragment distributions and multiplicities may not be sufficient to clarify the interplay of the stringlike collective degrees of freedom and that of the partonic ones.

In the dynamical string model all kinds of broken line string excitations are taken into account whereas, in other existing models, stringlike excitations are basically longitudinal and yo-yo-like, as long as no gluon jets (or minijets) are included. The dynamical string model has a rather few number of parameters as compared to other existing models. That is an advantage but, on the other hand, one cannot expect that the model in this form can provide more than an overall qualitative description of ultrarelativistic heavy-ion collisions.

In Sec. II we give a description of the dynamical string

model, and in Sec. III the model is applied to the ultrarelativistic heavy-ion collision ^{32}S(200 GeV/nucleon)+^{32}S.

II. DYNAMICAL STRING MODEL

A. Motivation

The underlying idea of the dynamical string model [19] is that hadrons can be represented by classical one-dimensional objects, the oriented relativistic open bosonic strings as suggested by Artru [20] and Remler [21]. There is experimental evidence that hadrons have stringlike collective degrees of freedom: (i) the well-known, almost linear Regge-trajectories [22] corresponding to the string tension of $\kappa \approx 0.9$ GeV/fm, (ii) the nearly exponential mass spectrum of the resolved hadron resonances [23], (iii) the existence of a preferred (longitudinal) direction in elementary fragmentation processes, (iv) the emission of linearly polarized gluons by the excited hadronic system occurring in high-energy *pp* collisions [24]. Theoretical indications and successful applications of the string model for hadronic physics are overviewed in [25]. For our work, the success of the string fragmentation models developed by Artru and Mennessier [26], and by the Lund group [6] was particularly encouraging. The oriented relativistic open string is thought of as the idealization of the chromoelectric flux tube with quark and antiquark (diquark) ends for mesons (baryons). The endpoints are assumed to have vanishing rest masses. The original idea is then modified; the infinitesimally thin strings have been replaced with more realistic thick ones, i.e., with strings exhibiting a finite tranverse size, more precisely a radius R. The hadronic strings introduced in this manner are treated afterwards in a fully dynamical way in our model. They propagate, collide, and decay according to the particular laws deduced from the string picture and from the analogy of hadronic strings with chromoelectric flux tubes, as described below.

Energy and momentum conservations are strictly satisfied in any elementary decay and collision event, and in the evolution of the whole hadronic system as well. No spin is introduced and the angular momentum conservation is not considered.

B. Mass spectrum

Our starting point is the classical Nambu-Goto string [27,28]. The classical mechanical string picture provides us with a continuous mass spectrum. All kinds of broken line string configurations can arise during the evolution of any system of hadronic strings due to inelastic string collisions. Furthermore, it has also been shown that those broken line string configurations with an arbitrary number of kinks are unavoidable to obtain a realistic exponential mass spectrum of hadronic strings [29]. A finite amount of momentum (and energy) can be carried by the kinks and by the string endpoints as well.

In order to be more realistic, below the mass thresholds of 1.5 GeV for baryons and 1.0 GeV for mesons strings, only those with discrete rest masses taken from [30] are allowed in the model. Strings in the rotating rod mode are associated with the discrete hadronic states, which correspond to the leading Regge trajectories [20]. It holds $2M = \kappa \pi l$ for their lengths l and rest masses M leading, e.g., to $l \sim 0.7$ fm for the nucleon, and $l \sim 0.1$ fm for the pion. Particles containing strange valence quarks are completely neglected.

The string endpoints carry the appropriate baryonic charges, and baryon number conservation is satisfied. Spin of the hadronic strings, electric charges, and flavors of the string endpoints have not been introduced. On the other hand, the degeneracies of the discrete resonance states due to their spin and isospin are taken into account.

C. Free motion

Any string configuration can be encoded in the trajectory of one of the endpoints of the string, in the so-called directrix [20], and boosted to any requested velocity as described in [19] in detail. The directrix determines the string configuration at a given time and also its free evolution according to the Nambu-Goto action. Any influence of the assumed transverse size of the hadronic strings on their free motion is neglected. During the evolution of the investigated system, each hadronic string is assumed to move freely between the subsequent elementary interaction events (decays and collisions) of its life.

In the numerical code the directrix is stored in less than 200 points, with typically 0.1 GeV rest mass for every linear segment of the broken line string. Whenever it is needed for describing single decay and collision events, the string can be constructed from its directrix unambiguously [20,19]. The string endpoints generally carry a finite amount of momentum, and are described by two string points at the same spatial position, but corresponding to different values of the string parameter [19].

In order to simulate any individual elementary string interaction event, the participating strings are reconstructed numerically from their directrices. After carrying out a single decay or collision event the final state strings must be converted back in their directrices. Generally, the conversion directrix $\rightarrow$ string $\rightarrow$ directrix leads to a doubling of the directrix points with many redundant ones that have to be removed by a reduction algorithm. If the endpoints of two neighboring directrix segments are almost on a straight line (i.e., the common point of both segments is rather close to one of the endpoints, or to the straight line connecting the endpoints), the segments are replaced by a single linear directrix segment under the constraint that energy and momentum must be conserved.

D. String collision

In the dynamical string model the collision is introduced as a binary interaction of strings. In order to obtain realistic total cross sections for the string-string collisions, a finite transverse size or radius R has to be prescribed to the hadronic strings as already established in [19]. This radius is chosen to be identical for all hadronic strings and it is also assumed not to be Lorentz contracted [31]. Strings coming in touch, and remaining after a critical collision time τ_c, still closer than their interaction range $2R$, interact. The total cross section is assumed to have a purely geometrical origin.

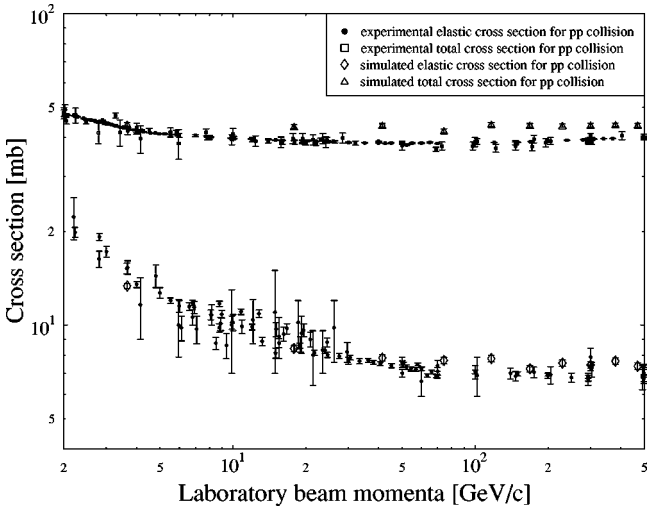

FIG. 1. Simulated total and elastic cross section for pp collision at different beam momenta.

Elastic and inelastic string-string collisions are distinguished, based also on geometrical concepts. An inelastic interaction range $R' < R$ is defined. Strings that are closer than $2R'$ after the time τ_c elapsed, since they came in touch, suffer inelastic collision, whereas the peripheral collisions are considered to be elastic ones. If the strings came in touch, but after the time τ_c they are at a distance larger than $2R$, they do not interact.

The differentiation between elastic and inelastic processes described above was tested by a numerical simulation of proton-proton (pp) collisions in the energy range $\sqrt{s}=3-30$ GeV (see Fig. 1). For determining the total and elastic pp cross sections, 10^4 collision events were numerically simulated by shooting a projectile proton ($N_p=1$) onto a target proton ($N_t=1$) at rest with an impact parameter $\leqslant \rho$. That is to say, the center of the target proton was positioned on the beam axis; the centers of the projectiles were uniformly distributed on a disk of radius $\rho \approx 1$ fm centered on the beam axis in the transverse plane. The initial states of the protons were represented by rotating rod modes. The orientations of the projectile and the target protons were uniformly distributed in the entire solid angle. Projectile protons were produced at a longitudinal distance 3 fm from the target. The simulations were performed by using the time steps $\Delta t = 0.02$ fm/c. The numbers N_{tot} and N_{el} of events with interaction and with elastic collision, respectively, were counted and converted to the corresponding total and elastic cross sections, $\sigma_{tot} = \rho^2 \pi N_{tot}/(N_t N_p v_p)$ and $\sigma_{el} = a^2 N_{el}/(N_t N_p v_p)$ with the projectile velocity v_p.

It is more involved (and also more time consuming) to calculate the distance of two strings than to determine the distance of two point particles. The distance d of two colliding strings is defined as the minimal distance of the points of a projectile string a and those of the target string b. The distance d is monitored for each string pair a and b in every time step as follows.

The distance between strings a and b can be estimated as $d_{est} = |\vec{x}_a - \vec{x}_b| - \frac{1}{2}(l_a + l_b)$, where $\vec{x}_{a,b}$ are the centers of mass and $l_{a,b}$ are the lengths of the strings a and b, respectively. If d_{est} is larger than the string interaction range $2R$, then d_{est} is taken for the distance of the string pair. Otherwise, the real distance d is computed. If once the real distance d is calculated for a string pair and turns out to be larger than the interaction range, $d > 2R$, it is not checked up to the time $t = (d-2R)/2c$ with c as the speed of light.

After the strings came in touch, i.e., their distance became $d(t_0) \leqslant 2R$ at time t_0, they can interact. The decisions on the interaction and on the interaction channel (if any) are taken after a critical time τ_c elapsed. There is no interaction if the distance of the strings $d(t_0+\tau_c) > 2R$, while an elastic collision or an inelastic collision takes place if $2R > d(t_0+\tau_c) > 2R'$ or $d(t_0+\tau_c) < 2R'$, respectively.

It was concluded that the elastic and inelastic cross sections shown in Fig. 1 are in qualitative agreement with experimental data for the interaction ranges $R \approx 0.6$ fm and $R' = 0.7R \approx 0.4$ fm, and the interaction time $\tau_c = 0.4$ fm/c. The ratio of the simulated elastic and total cross sections, and the energy dependence of the elastic cross section are rather sensitive to the ratio R'/R and to τ_c. The simulated results are consistent with the following order of magnitude estimates valid for large values of the projectile momentum: $\sigma_{tot} \to 4R^2\pi \approx 45$ mb and $\sigma_{el} \to 4(R-R')^2\pi \approx 5$ mb. These estimates do not take into account the orientations of the strings. There is a difference of the results obtained here ($\sigma_{tot} = 45$ mb for $R = 0.6$ fm) and in [19] (the same σ_{tot} for $R = 0.45$ fm). It is the consequence of introducing the interaction time τ_c. Strings overlapping only at their ends for a short time may leave their interaction range during the time τ_c after having come in touch.

In the dynamical string model the distance of any pair of strings must be determined in every time step with the algorithm described above. A great amount of computational time can be spared in the simulation of heavy-ion collisions by determining the estimate d_{est} and not calculating the actual distance for $d_{est} > 2R$. Once, in the simulation of a heavy-ion collision event, a string pair came in touch and the time τ_c is over, the channel of the collision (inelastic, elastic, or no interaction) is decided as described above and the appropriate final state in the actual collision channel is generated.

In the simulations presented here, the elastic channel is introduced only to reduce the inelastic fraction of the total cross section, but the strings that suffered an elastic collision were let to move further as if nothing had happened.

The inelastic collisions are considered rearrangements [20]. The rearrangement of infinitely thin colliding strings is a simple cut followed by the reconnection of the string arms at the point of intersection. The order of the reconnection is always unique, as the strings are oriented objects. In the numerical code the rearrangement is carried out in the time step when the interaction time τ_c after the strings came in touch is over, and the criterium $d < 2R'$ is fulfilled. Then the points of the minimal distance define the points where the strings are disjoined and reconnected once again. The reconnection is performed by displacing the appropriate string pieces. Energy and momentum are conserved automatically, and the center of energy of the string pair is conserved by displacing the string pair as a whole appropriately. Owing to the interaction time τ_c, the new strings generally can move away, so

that any undesired infinite sequence of interactions is avoided.

According to the above prescription of rearrangement for a string with continuous mass spectrum, it may happen that one or both of the final state strings would have rest masses below the mass thresholds. Similar final states could also arise as a result of decay. Their treatment shall be discussed later in detail. A collision of discrete resonances or that of a discrete resonance with a string of the continuous mass spectrum are treated according to the same rules as the collisions of the strings of the continuous mass spectrum, as the resonances are represented by strings in the rotating rod mode.

E. Decay

The decay law for relativistic strings belonging to the continuous mass spectrum is given by $dw=-\Lambda dA$, i.e., the probability dw that the string piece having swept the invariant area dA breaks is proportional to that area, with the decay constant Λ [26]. Making use of the analogy of the hadronic string with the chromoelectric flux tube, the decay is considered the result of the production of a quark-antiquark pair via the tunneling effect in the strong chromoelectric field of the flux tube [32]. Then the decay constant $\Lambda=R^2\pi w(R)$ can be expressed in terms of the quark-antiquark pair production rate $w(R)$ depending on the radius of the flux tube [34,33]. The created quark and antiquark acquire oppositely directed transverse momenta with an approximately Gaussian distribution $dP(p_T)\sim\exp(-p_T^2/2p_{T0}^2)dp_T^2$ $(p_{T0}\approx 1.43/R)$, deduced from the analogy with flux tubes [35].

The decay of strings with rest masses above the threshold is simulated as follows. For any string created, an invariant area A_0 is chosen according to the distribution $\sim\exp(-\Lambda A_0)$. The increment of the invariant area swept by the string is calculated in every time step as the sum of area elements of the linear string segments. In the time step when the invariant area swept by the string exceeds the value A_0, the string is broken up without any time delay. The decay is performed in the segment for which the probability of decay has a maximum for that time step. The transverse momenta of the new string ends are chosen with the distribution $dP(p_T)$, and with uniform distribution in the plane transverse to the decaying string piece in its rest frame. A piece of the string is removed around the breaking point that is required to satisfy energy and momentum conservation.

The decay of discrete resonances is not considered like a string decay. Their lifetimes and decay channels are taken from [30]. According to the exponential decay law of point particles, a time T_0 is chosen for every resonance created, and having that elapsed, its decay is performed.

The decay of discrete resonances can result in two or three daughters. For decay into two daughters the magnitudes of their momenta are well defined, and the direction of the momenta is chosen isotropically in the rest frame of the mother resonance. For decay into three daughters it is assumed that the momenta of the daughters lie in a plane of randomly chosen orientation in the rest frame of the mother resonance, the momenta are of equal magnitude, and each neighboring pair closes the angle 120° in the rest frame of the mother. The direction of one of the three momenta are chosen isotropically in the plane. The magnitudes of the momenta determined under these assumptions from energy conservation are in agreement with the average momenta indicated in [30]. Finally, the daughter resonances are represented by the appropriate rotating rods, displaced out of their interaction range in the directions of their momenta.

F. Final states with discrete resonances

Both the rearrangement and decay of strings, belonging to the continuous mass spectrum, can result in two-particle final states with one or both strings below the mass threshold. These cases are treated in the model in different ways.

(1) The case with two rest masses below the threshold is considered a final state with two discrete resonances. The pair of resonances is chosen randomly according to the degeneracies of the resonances, under the restriction that the sum of the rest masses of the resonance pair must not exceed the invariant mass of the colliding string pair (of the mother string). Then the momenta of the resonances are chosen randomly with isotropic orientation in the rest frame of the pair, satisfying energy and momentum conservation. Finally, the resonances are represented by rotating rods with the appropriate rest masses and momenta, and are displaced in the direction of their momenta out of their interaction range conserving the center of energy of the pair.

(2) The case with one rest mass m_r below the threshold is considered a final state with one discrete resonance and a string belonging to the continuous part of the mass spectrum. The resonance is chosen randomly taking the degeneracies into account, under the restriction that the sum of the rest masses of the final state particles must not exceed the invariant mass of the initial strings (of the mother string). Further on, one has to proceed differently for rearrangement and for decay.

1. For rearrangement

One has to distinguish the cases with a mesonic or baryonic string occurring below the corresponding mass threshold.

(i) Meson below the mass threshold. If the rest mass m_r below the mesonic threshold M_M turned out to be smaller than the pion mass, $m_r<m_\pi$, the colliding strings are considered to fuse in a single one. If $m_\pi<m_r<M_M$, the resonance with rest mass $M_r<m_r$, but closest to m_r, is chosen with the same momentum $\vec{P}_r$, which is what the string with rest mass m_r would have had. The other string is slightly modified by chopping off its wedge at the point of reconnection and inserting a linear segment of vanishing momentum with rest mass m_r-M_r.

(ii) Baryon below the mass threshold. Then the possibility of the fusion of both colliding strings is excluded in order to avoid exotic many quark states. Therefore, even if m_r is smaller than the nucleon mass, $m_r<m_N$, the proton is chosen for the discrete state. The construction of the final state is performed similarly to that for a discrete meson and a string. The mass difference m_N-m_r, however, is now taken away

TABLE I. Parameter sets used for the simulations of heavy-ion collision events.

Parameter set	κ (GeV/fm)	R (fm)	R' (fm)	ν	σ_{tot} (mb)	Λ (fm^{-2})	T_l (fm/c)
(a)	0.9	0.6	0.42	2.0	45	1.25	0.8
(b)	0.9	0.5	0.35	1.5	31	0.14	2.2

from the other string by chopping off its wedge and displacing its arms to bring them in connection at their new endpoints. Otherwise, for $m_N<m_r<M_B$ (with the baryonic threshold M_B), the final state is constructed in the same way as for a discrete meson state and a string.

2. For decay

The smallest possible piece at the end of the continuous string is chopped off that is required to satisfy energy and momentum conservation for the final state, when the resonance and the new string endpoint acquire the transverse momenta $\vec{p}_T$ and $-\vec{p}_T$, respectively. The transverse momenta are chosen randomly according to the distribution $dP(p_T)$, and oriented isotropically in the plane perpendicular to the string at its endpoint. Finally, the discrete resonance is represented by the corresponding rotating rod and positioned so that the centers of energy of the initial and final states must be identical.

G. Parameters

There are relatively few parameters in our model. The dynamical string model has two basic parameters: the string tension $\kappa \approx 0.9$ GeV/fm fitted to the slopes of the leading Regge trajectories, and the string radius $R \approx 0.6$ fm, fitted to the total proton-proton cross section. The ambiguity in the analogy of strings with chromoelectric flux tubes results in a factor of $\nu=2$ uncertainty in the relation between the string tension κ and the product of the color charge e of the quark and the field strength $\mathcal{E}$, $\nu\kappa=e\mathcal{E}$ with $\nu \in [1,2]$ [35]. Two more parameters are the ratio of the inelastic range R' to the full radius R of the string: $R'/R \approx 0.7$ and the collision time $\tau_c=0.4$ fm/c fitted to the total and elastic proton-proton cross sections. Furthermore, the masses, degeneracies, and lifetimes taken from [30] have been used for the discrete resonances below the mass thresholds, and the mesonic and baryonic mass thresholds $M_M=1.0$ GeV and $M_B=1.5$ GeV have been chosen.

According to the analogy of the hadronic strings with the chromoelectric flux tubes, the decay constant Λ of the string is determined by the parameters κ, R, and ν [35]. In Table I we list the parameter sets used for the simulation of heavy-ion collision events, also including the corresponding total proton-proton cross sections at high energies and the decay constants and mean lifetimes (T_l) of the strings. The mean lifetimes are determined for the so-called yo-yo mode [20] according to the exponential decay law, $T_l=\sqrt{(\ln 2)/\Lambda}$.

The dynamical string model with the parameter sets given in Table I has been tested by simulating elementary hadronization processes: two-jet events in $e^+e^- \rightarrow hadrons$ at c.m. energies of 20–50 GeV [35,36] and hadronization in proton-proton collisions at 29 and 200 GeV bombarding energies [37,38]. The parameter set (a) is consistent with the total proton-proton cross sections. It provides a decay constant for which the simulated results on the Bose-Einstein correlation of like-sign pions and on the average charged particle multiplicity are in good agreement with experimental data for $e^+e^- \rightarrow hadrons$ [36,39]. Simulated results for the single-particle distributions for the same process [36] and for the proton-proton collisions [37,38] are also in good qualitative agreement with the corresponding data, but the average charged particle multiplicity in proton-proton collisions is overestimated by nearly 40%.

The parameter set (b) has been found the optimal one in the simulation for reproducing the single-particle data on $e^+e^- \rightarrow hadrons$ [35], but it leads to an unrealistically small value of the string decay constant and practically no Bose-Einstein correlation of like-sign pions occurs in the simulation [36] using this set. Furthermore, the total proton-proton cross section for high energies is underestimated by the parameter set (b) as seen in Table I. Single-particle data on proton-proton collisions can be described with a quality similar to that of the corresponding results for parameter set (a), with a similar overestimate of the average charged particle multiplicity. It should be mentioned that according to the calculations in [35] the parameters of the set (a) are not optimal but still in the range which is acceptable for describing the single-particle distributions in $e^+e^- \rightarrow hadrons$. Thus, the parameter set (a) is preferred on the basis of comparing the simulated results with experimental data on the elementary hadronization processes considered above.

The mean lifetime 0.8 fm/c of strings for parameter set (a) is close to the value of 1.2 ± 0.1 fm/c determined in [40]. On the other hand, the string radius $R=0.6$ fm of parameter set (a) is also consistent with the range of its value (0.5

TABLE II. Average multiplicities $\langle h^- \rangle$ of negatively charged hadrons and the average multiplicities per total baryon number B for various colliding systems. The simulated data are presented for both parameter sets (a) and (b). Here the same number of net baryons (B) is assumed as was measured in the experiment S+S. The experimental data are taken from [42].

	System (lab. energy/nucleon)	$\langle h^- \rangle$	$\langle h^- \rangle / B$
Experiment	S + S (200 GeV/nucleon)	95 ± 5	1.8 ± 0.2
Experiment	S + Ag (200 GeV/nucleon)	160 ± 8	1.8 ± 0.2
Simulation (a)	^{35}N+^{35}N (200 GeV/nucleon)	126 ± 9	2.4 ± 0.3
Simulation (b)	^{35}N+^{35}N (200 GeV/nucleon)	128 ± 11	2.4 ± 0.3

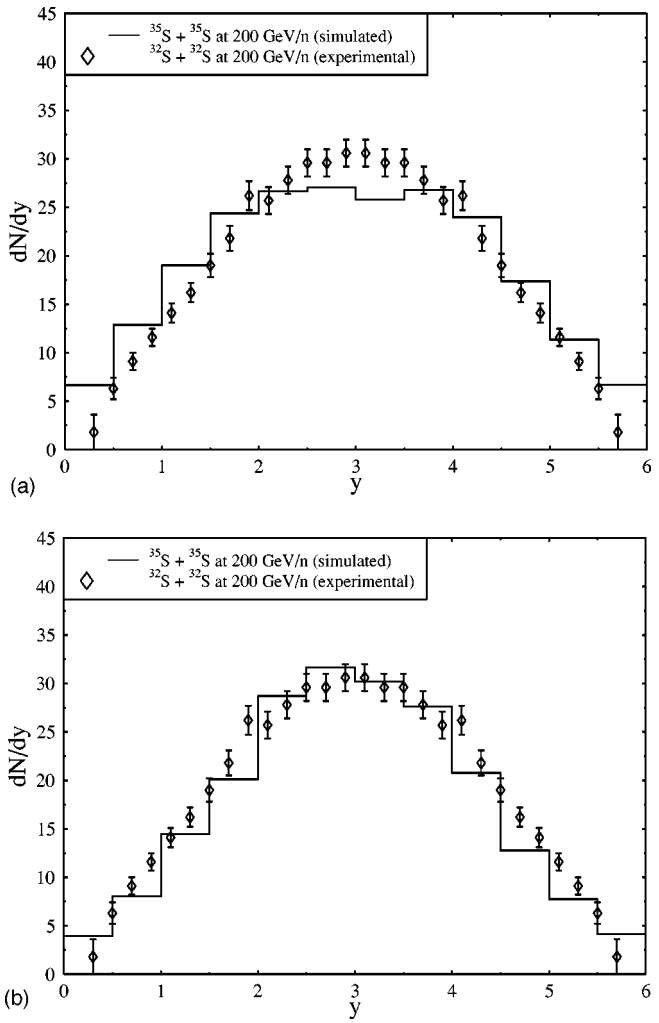

FIG. 2. Rapidity distributions of negatively charged hadrons for parameter sets (a) and (b).

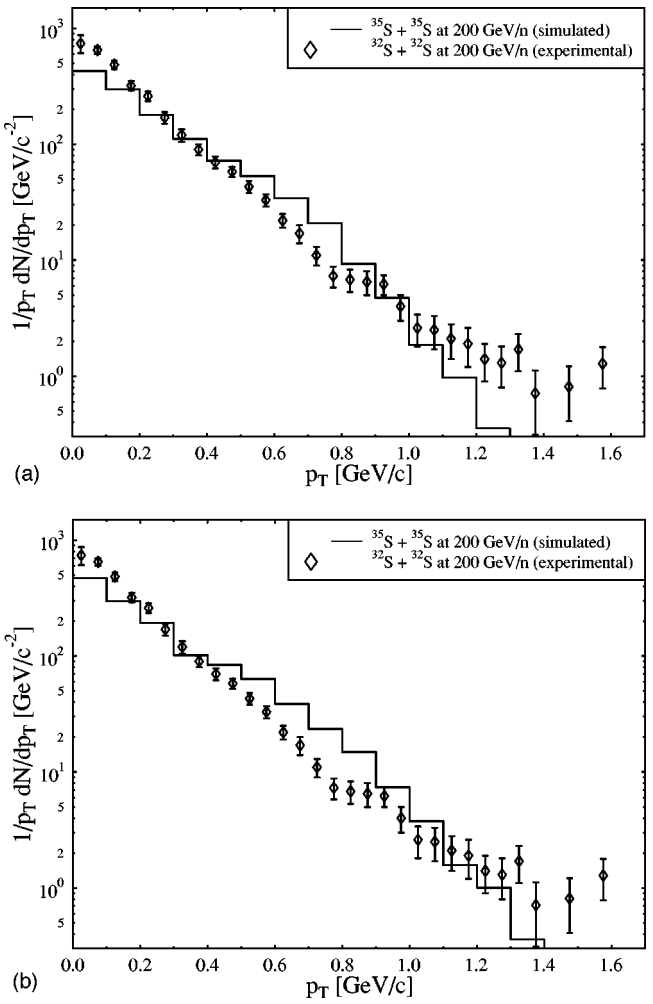

FIG. 3. Transverse momentum distributions of negatively charged hadrons for parameter sets (a) and (b).

± 0.1) fm, which was established on the basis of the experimentally observed strangeness fraction in proton-proton collision [34].

III. SIMULATION OF ULTRARELATIVISTIC HEAVY-ION COLLISIONS

The dynamical string model described above has been applied to the simulation of ultrarelativistic heavy-ion collision events. For both parameter sets 250 collision events were simulated. Hypothetical nuclei of mass number $A=35$ shooted on one another in the c.m.s. were constructed in the following way. The centers of the nucleonic strings (rotating rods of length 0.7 fm) were positioned at the nodes and the centers of the cells of a cubical 3^3 lattice with lattice spacing 2.1 fm drawn in a sphere of the nuclear radius $R_A = r_0 A^{1/3} = 3.6$ fm ($r_0 = 1.1$ fm). The Fermi motion of the nucleons has been neglected; their orientations were chosen randomly according to a uniform distribution in the entire solid angle. Two such ''cubes'' with parallel edges were boosted to the appropriate c.m.s. momenta. Central collisions with impact parameters less than 2 fm were considered. The center of one of the nuclei was chosen according to a uniform distribution in the transverse plane, within a circle of radius of 2 fm around the projection of the center of the other nucleus to that plane. Constructing the hypothetical nuclei in a cubic configuration gives an extra periodic structure of the nucleus instead of the fluidlike random one. On the other hand the possible effect of this periodicity is completely neutralized by choosing different impact parameters for the individual collision events randomly. In the numerical simulation no side effects originating from the periodic configuration were seen.

The simulations were performed with the same time steps of $\Delta t = 0.02$ fm/c as used to fit the total and inelastic radii of the strings and to perform the test simulations. It is rather important to take into account the elastic string-string collisions, since the secondary collisions in ultrarelativistic heavy-ion collisions play a distinguished role.

The simulations were performed with both parameter sets (a) and (b). The simulated results were transformed back to the laboratory system and compared with experimental data on $^{32}S + ^{32}S$ central collisions at the bombarding energy of 200 GeV/nucleon in the NA35 experiment at CERN [41,42].

In order to take into account the difference between the mass numbers of the nuclei in the simulation and the experiment, the simulated distributions were systematically renormalized by the factor $(32/35)^2$.

The average multiplicities of the produced hadrons with negative charge (supposed to be π^- in the experiment) are compared to the simulated results in Table II. Since the dynamical string model does not account for electric charges, one third of the produced mesons is assumed to be negative based on isospin arguments. The simulated average multiplicity of negatively charged particles is overestimated by about 30% as compared to the multiplicity in the reaction $^{32}S+^{32}S$. This can also be seen from the data for the averaged negative charged particle multiplicity per participating baryons, which varies slightly for different mass numbers [42]. The overestimate can be the consequence of overestimating the multiplicities in individual string-string collisions, as test simulations for proton-proton collisions have shown. Also the complete neglection of the strangeness channel and the rather crude treatment of elastic string-string collisions can affect the average charged particle multiplicity.

The rapidity and the transverse momentum distributions of negatively charged hadrons are shown in Figs. 2 and 3, respectively. It can be seen that the experimental spectra are reproduced by the model for both parameter sets qualitatively.

IV. CONCLUSIONS

The dynamical string model has been generalized in order to simulate ultrarelativistic heavy-ion collisions at current collider energies. The initialization of the incoming nuclei and the discrimination of the elastic and inelastic scattering of strings are now included. An effective optimization of the collision algorithm has been performed in the numerical code. In this way, the model is able to simulate nucleus-nucleus collisions at beam energies of a few hundreds of GeV/nucleon for nuclei with mass numbers up to around 40. The simulated results for the reaction $^{32}S+^{32}S$ at a beam energy of 200 GeV/nucleon are in good qualitative agreement with the experimental data. Therefore, the dynamical string model has a predictive power for ultrarelativistic heavy-ion collisions.

ACKNOWLEDGMENTS

This work was supported by the Debrecen Research Group in Physics of the Hungarian Academy of Sciences, by OTKA Project No. T-023844, DFG Project No. 436/UNG/113/123/0, the GSI, and BMBF. The authors are grateful to W. Greiner for his kind hospitality at the Institute for Theoretical Physics, Johann Wolfgang Goethe University. K. Sailer is thankful for the support of the Alexander von Humboldt Foundation. B. Iványi wishes to express his thanks to the DAAD for their support.

[1] T. Sjöstrand, Comput. Phys. Commun. **82**, 74 (1994).
[2] G. Marchesini, B. R. Webber, G. Abbiendi, I. G. Knowles, M. H. Seymor, and L. Stanco, Comput. Phys. Commun. **67**, 465 (1992).
[3] L. Lönnblad, Comput. Phys. Commun. **7**, 15 (1992).
[4] G. Ingelman, A. Edin, and J. Rathsman, Prep. DESY-96-057 (1996); hep-ph/9605286.
[5] F. Paige and S. Protopopescu, in *Supercollider Physics*, edited by D. Soper (World Scientific, Singapore 1986); H. Baer, F. Paige, S. Protopopescu, and X. Tata, in *Proceedings of the Workshop on Physics at Current Accelerators and Supercolliders*, edited by J. Hewett, A. White, and D. Zeppenfeld (Argonne National Laboratory, Argonne, Illinois, 1993).
[6] B. Andersson, G. Gustafson, G. Ingelmann, and T. Sjöstrand, Phys. Rep. **97**, 33 (1983); B. Andersson, G. Gustafson, and B. Söderberg, Nucl. Phys. **B264**, 29 (1986).
[7] B. Andersson, G. Gustafson, and B. Nilsson-Almquist, Nucl. Phys. **B281**, 289 (1987); B. Nilsson-Almquist and E. Stenlund, Comput. Phys. Commun. **43**, 387 (1987); B. Lörstad, Int. J. Mod. Phys. A **2**, 2861 (1989).
[8] K. Geiger and B. Müller, Nucl. Phys. **B369**, 660 (1992); K. Geiger, Phys. Rep. **258**, 237 (1995).
[9] A. Capella, U. Sikhatme, C.-I. Tan, and J. Tran Tranh Van, Phys. Rep. **236**, 225 (1994).
[10] K. Werner, Z. Phys. C **42**, 85 (1989); Phys. Rep. **232**, 87 (1993).
[11] L. V. Bravina, N. S. Amelin, L. P. Csernai, P. Lévai, and D. Strottman, Nucl. Phys. **A566**, 461c (1994).
[12] H. Sorge, H. Stöcker, and W. Greiner, Nucl. Phys. **A498**, 567c (1989); Ann. Phys. (N.Y.) **192**, 266 (1989).
[13] S. A. Bass, M. Belkacem, M. Bleicher, M. Brandstetter, L. Bravina, C. Ernst, L. Gerland, M. Hofmann, S. Hofmann, J. Konopka, G. Mao, L. Neise, S. Soff, C. Spieles, H. Weber, L. A. Winkelmann, H. Stöcker, W. Greiner, Ch. Hartnack, J. Aichelin, and N. Amelin, Prog. Part. Nucl. Phys. **41**, 225 (1998); nucl-th/9803035.
[14] W. Ehehalt and W. Cassing, Nucl. Phys. **A602**, 449 (1996); hep-ph/9507274.
[15] A. Shor and R. Longacre, Phys. Lett. B **218**, 100 (1989).
[16] X. N. Wang and M. Gyulassy, Phys. Rev. D **44**, 3501 (1991); Comput. Phys. Commun. **83**, 307 (1994).
[17] D. E. Kahana and S. H. Kahana, Phys. Rev. C **58**, 3574 (1998).
[18] K. Geiger, R. Longacre, and D. K. Srivastava, Comput. Phys. Commun. **104**, 70 (1997).
[19] K. Sailer, B. Müller, and W. Greiner *Quark-Gluon Plasma*, edited by R. C. Hwa (World Scientific, Singapore, 1990), p. 299.
[20] X. Artru, Phys. Rep. **97**, 147 (1983).
[21] E. A. Remler, *Proceedings of the XV International Workshop on Gross Properties of Nuclei and Nuclear Excitations*, Hirschegg, Austria, 1987 (GSI, Darmstadt, 1989), p. 24; *Proceedings of the XVII International Workshop on Gross Properties of Nuclei and Nuclear Excitations*, Hirschegg, Austria, 1989 (GSI, Darmstadt, 1989), p. 184.
[22] P. D. B. Collins, Phys. Rep. **1**, 105 (1971).
[23] R. Hagedorn, Nuovo Cimento Suppl. **3**, 147 (1965).

[24] T. Jacobsen and H. A. Olsen, Phys. Scr. **42**, 513 (1990).
[25] K. Sailer, Th. Schönfeld, Z. Schram, A. Schäfer, and W. Greiner, J. Phys. G **17**, 1005 (1991).
[26] X. Artru and G. Mennessier, Nucl. Phys. **B70**, 93 (1974).
[27] Y. Nambu, Lecture at Copenhagen Summer Symposium (1970); O. Hara, Prog. Theor. Phys. **46**, 1549 (1971); T. Goto, *ibid.* **46**, 1560 (1971).
[28] B. F. Hatfield, *Quantum Field Theory of Point Particles and Strings* (Addison-Wesley, Reading, MA, 1992).
[29] K. Sailer, B. Müller, and W. Greiner, Int. J. Mod. Phys. A **4**, 437 (1989).
[30] Particle Data Group, L. Montanet *et al.*, Phys. Rev. D **50**, 1173 (1994).
[31] J. D. Bjorken, in *Current-Induced Reactions*, edited by J.D. Körner, G. Kramer, and D. Schildknecht (Springer, New York, 1976), p. 93.
[32] A. Casher, H. Neuberger, and S. Nussinov, Phys. Rev. D **20**, 179 (1979); E. Gurvich, Phys. Lett. **87B**, 386 (1979); N. K. Glendenning and T. Matsui, Phys. Rev. D **28**, 2890 (1983).
[33] H. P. Pavel and D. M. Brink, Z. Phys. C **51**, 119 (1991).
[34] Th. Schönfeld, A. Schäfer, B. Müller, K. Sailer, J. Reinhardt, and W. Greiner, Phys. Lett. B **247**, 5 (1990).
[35] Th. Schönfeld, A. Schäfer, B. Müller, K. Sailer, J. Reinhardt, and W. Greiner, Phys. Lett. B **240**, 381 (1990).
[36] B. Iványi, Zs. Schram, K. Sailer, and W. Greiner, Acta Phys. Hung. New Ser.: Heavy Ion Phys. **3**, 5 (1996); hep-ph/9510380.
[37] B. Iványi, Zs. Schram, K. Sailer, and W. Greiner, in *Hot and Dense Nuclear Matter*, Proceedings of NASI, Bodrum, 1993, edited by W. Greiner (Plenum, New York, 1994), p. 751.
[38] B. Iványi, Zs. Schram, K Sailer, and W. Greiner, Proceedings of Hadrons '94 Workshop Uzsgorod, Ukraine 1994 (ITF NAN, Kiev, 1994), p. 240.
[39] H. Aihara *et al.*, Phys. Rev. D **31**, 996 (1985).
[40] W. Busza, T. Dreyer, and M. Erdmann, Z. Phys. C **48**, 167 (1990).
[41] J. W. Harris *et al.*, Nucl. Phys. **A498**, 133c (1989).
[42] D. Röhrich *et al.*, Nucl. Phys. **A566**, 35c (1994).